5-2022

Using fluorescent microscopy to follow mitochondrial Inheritance through tagged alternative oxidase in sporisorium reilianum.

Luke Schroeder
University of Louisville

USING FLUORESCENT MICROSCOPY TO FOLLOW MITOCHONDRIAL INHERITANCE THROUGH TAGGED ALTERNATIVE OXIDASE IN *SPORISORIUM REILIANUM*

By

Luke Schroeder

Submitted in Partial Fulfillment of the Requirements for Graduation *summa cum laude*

University of Louisville

Louisville, Kentucky

March, 2022

Abstract

Sporisorium reilianum is a dimorphic fungus that inhabits and infects a host corn plant (*Zea mays*). In order for the fungus to reproduce sexually, compatible haploid mating types must form a dikaryon that goes on to cause infection in the host. This infection causes leaf chlorosis and gall formation, while ultimately allowing for the dispersal of fungal teliospores in the later stages of infection. To grow, the fungus requires energy production in the form of ATP from its mitochondria. As a countermeasure to infection, host plants release harsh reactive oxygen species that may damage DNA, lead to apoptosis, and reduce the ability of organisms to produce ATP via the electron transport chain in the mitochondrion. The fungus may survive this assault by utilizing an alternative oxidase, which gives the fungi an alternative pathway in the electron transport chain. Thus, alternative oxidase (Aox) is a necessary part of the fungal mitochondria and will be highly expressed at some points during its life cycle. This leads to the unique opportunity to make use of the presence of Aox in the mitochondria and tag the protein fluorescently to track it, and also mitochondrial dynamics, throughout the fungal lifecycle. Fluorescent tagging will allow for a better understanding of fungal mitochondria and what happens to the mitochondria of fungi when sexual reproduction occurs between different mating types. This study serves to investigate the utility of fluorescently tagging Aox for the purpose of better understanding these mating-type interactions. Two mating partners 5-1 and 5-2 of *S. reilianum* were tagged and observed using confocal microscopy. The strains were then crossed and fusion was observed between the 5-1 mCherry #2 and 5-2 eGFP #6 strains.

1. Introduction

Sporisorium reilianum is a pathogenic basidiomycete with two variants capable of infecting maize (*S. reilianum* formae specialis *zeae*, or SRZ) and sorghum (*S. reilianum* formae specialis *reilianum*, SRS). Similar to the related species *Ustilago maydis*, SRZ has a haploid yeast-like sporidia stage where the fungus reproduces asexually via budding (Martinez, 2002). Later in its life cycle, SRZ is capable of sexual reproduction in which it utilizes a tetrapolar mating-type system. Tetrapolar refers to the presence of two separate regions in the genome that determine the mating type of the fungus. These unlinked mating loci (*a* and *b*) must each be different between mating strains such that a fungus with *a1b1* mating loci can sexually reproduce with another individual with, for example, *a2b2* mating loci (but not with *a1b2* or *a2b1*). The first step required for sexual reproduction to begin is that the mating types differ in the *a* locus that codes for pheromone-pheromone receptor genes. In SRZ, there are 3 different *a* locus types (a1-a3) which can each interact with each other. For example, the *a1* mating partner would create a pheromone that can only be recognized by the pheromone receptor expressed by the *a2* mating partner and vice versa. When the pheromone receptor of an SRZ cell binds to the pheromone of a potential mating partner, the fungal cell will begin to grow conjugation hyphae and search for the other cell releasing compatible pheromones. When they encounter each other, the SRZ cells must then determine if they differ at the *b* locus of which there are at least 5 identified allele variants. Assuming they differ at the *b* locus as well, the conjugation hyphae from both mating types then fuse together, which results in a new filamentous structure called a dikaryon, which is capable of infecting a plant cell (Schirawski, 2005). This pathogenic phase where the dikaryon differentiates and ultimately causes symptoms in the plant is a required step for sexual reproduction to occur in SRZ.

Unlike *U. maydis*, SRZ results in systematic host infection of the whole plant with severe symptoms in the late stages of the plant's life cycle. This infection leads to the formation of diploid teliospores inside tumor-like structures called galls. These teliospore structures can range from a few black dust-like spots to a large mass covering the tassel or cob. The dark pigmentation of these teliospores in the galls gives SRZ its name of "smut fungus". By supplanting the host's reproductive organs (tassel and cob) with its own teliospores, the fungus is able to make use of a preexisting host system to spread its genetic material to other susceptible maize plants in the area. Those diploid teliospores are then able to germinate under ideal conditions and restart the life cycle again as haploid sporidia. Beyond teliospores, the infection caused by SRZ can also result in chlorosis (yellowing of the leaves) and the production of anthocyanin, a pigment causing red or purple color changes in the leaves. (Martinez, 2002).

Due to its infectious nature, SRZ poses a risk to agricultural operations utilizing corn, however, advances in hybrid corn strains have diminished this threat. SRZ remains an effective model for host-pathogen interactions along with fungal mating and virulence. An especially interesting interaction between SRZ and its host occurs in the mitochondria of SRZ cells that the host attempts to disable.

Within many eukaryotic systems, the full function and inheritance patterns of mitochondria are not fully known. This is surprising considering the importance of the mitochondria and electron transport chain (ETC) for the production of energy in almost every living organism. The mitochondria, and ETC for fungal systems in particular, such as SRZ, are even less well studied. In eukaryotic organisms, the mitochondria are known to convert reduced carbon to a usable energy currency in the form of adenosine triphosphate (ATP). This is accomplished through generation of electron carriers during glycolysis and the tricarboxylic acid

cycle that go on to generate an electrochemical gradient at the ETC. The ETC itself is made up of four protein complexes including complex I (NADH ubiquinone oxidoreductase), complex II (succinate dehydrogenase), complex III (cytochrome bc1), and complex IV (cytochrome c oxidase) along with two intermediates: ubiquinone (Q) and cytochrome c. All the complexes except for complex II contribute to the formation of a proton motive force by pumping protons into the intermembrane space of the mitochondria. This pumping action of the complexes is powered by the movement of electrons from electron donors, NADH and $FADH_2$, to the terminal electron acceptor, molecular oxygen. (Juárez, 2004). Ultimately, ATP is produced when the protons pumped into the intermembrane space are able to flow back down their concentration gradient through ATP synthase and return to the mitochondrial matrix.

Beyond the general overview of the ETC and especially important to the host-pathogen interactions of SRZ are alternative respiratory components. These proteins serve a special role in multiple organisms ranging from the peanut plant to fungal pathogens of animals and plants. The alternative oxidase acts as an additional route in the ETC that doesn't make full use of all the complexes I through IV. This results in less proton pumping and thus less ATP but in plants, using these alternative pathways has been associated with thermotolerance (Grabelnych, 2014), along with chemical (Smith, 2009) and oxidative stresses (Dinakar, 2016). In *U. maydis*, alternative oxidase proteins help maintain homeostasis and allow the fungal mitochondria to continue substrate-level phosphorylation with a large waste of energy as heat (Juárez, 2006).

In SRZ, the alternative component is an alternative oxidase (Aox) that can serve as a terminal electron acceptor (Rogov, 2014). In the ETC, Aox comes right before complex III and IV and it can be used as a terminal electron acceptor instead of using the traditional path through complex III and IV to reach O_2. This loss of complex III and IV proton pumping action results in

a significant loss in protons pumped into the intermembrane space and thus total ATP production is significantly diminished. Even though Aox use results in a much lower net ATP production, it remains a valuable tool for SRZ to survive harsh conditions within the plant host. These conditions result from the host's defense system, which produces radical oxygen species (ROS) capable of inhibiting complex III and IV. If these complexes are blocked, no cycling of electron carriers can occur and all energy production ceases, which effectively kills SRZ, an obligate aerobe. The presence of Aox ensures that the respiration cycle can continue with molecular oxygen as a final electron acceptor in Aox. The fungus won't be able to produce normal amounts of ATP using the Aox method, but other systems like glycolysis and the TCA cycle, which also make small amounts of ATP, can continue to occur in the cell. This will allow SRZ to survive the harsh conditions in the plant due to ROS (Mendoza, 2022). Figure 1 shows a traditional ETC with included Aox protein.

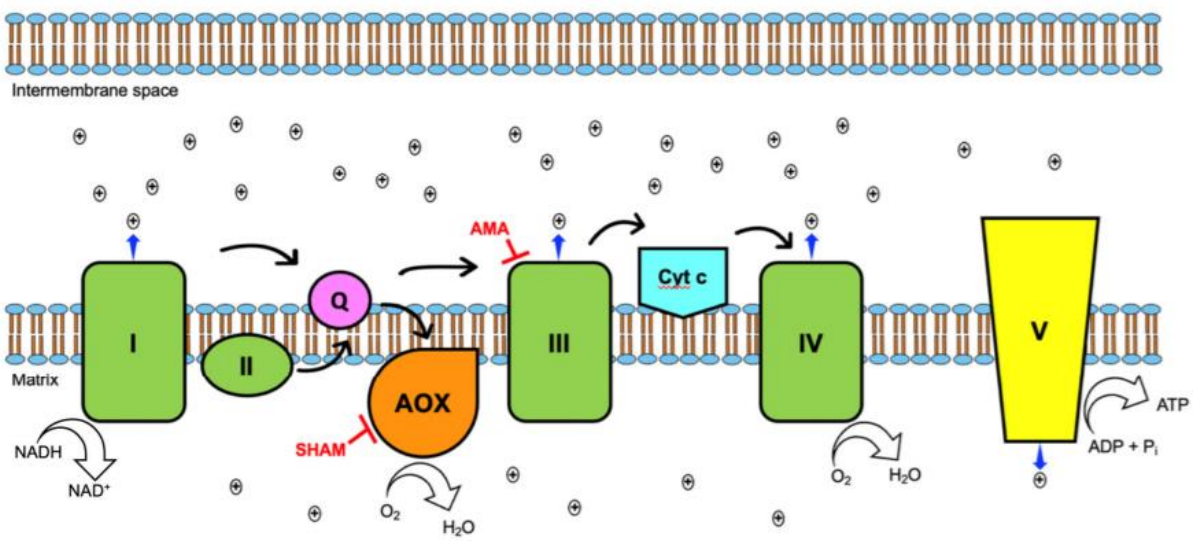

Figure 1. Electron transport chain (ETC) with included Aox. Black arrows indicate the movement of electrons through the ETC. The traditional electron pathway through complexes I-IV is shown in green. Protons are pumped into the intermembrane space by complex I, III, and IV as shown by the blue arrows. The pathway generates an electrochemical gradient that powers ATP synthesis via the flowing of protons through ATP synthase (complex V, in yellow). Aox is shown in orange and can act as a terminal electron acceptor as well, but with no ATP production (with permission from Mendoza, 2022).

Considering the importance of the Aox protein for resisting the host during the pathogenic part of SRZ's life cycle, it is likely that Aox will be highly expressed during sexual reproduction between haploid fungal strains. Similar to many other genes encoding mitochondrial components, the gene for Aox is located in the nucleus. After the gene is transcribed and translated, the Aox protein localizes into the inner membrane of the mitochondria. If the wild type gene was replaced with a modified version encoding Aox fused with a fluorescent protein, the tagged Aox would end up in the mitochondria. These characteristics make Aox a good target for tagging with the purpose of mitochondrial visualization. This fluorescent protein could then be tracked using microscopy to gain a better understanding of fungal mitochondria. Additionally, the alteration being present in the genome of the cell means that it can be passed on to the cell's offspring. Those offspring would then have fluorescent mitochondria in the same way as their parent cells.

Like numerous other organisms, including humans, SRZ and related fungi, appear to have a genetic mechanism in place to control the inheritance of mitochondria after mating. Human egg cells provide most, if not all, mitochondria after fertilization (Giles, 1980), in part due to the extreme difference in size between egg and sperm cells. If it mimics its close relative, *Ustilago maydis*, SRZ should also be able to control mitochondrial inheritance after mating. Since it bears orthologues of the genes required in *U. maydis* (Figure 2) for such control (*i.e.*, *lga2* and *rga2*), SRZ would be predicted to preferentially retain a2 mitochondria in the dikaryon (Fedler, 2009). This is true even though the participants in such mating are cells of equal size, unlike the case for sperm and egg cells. Thus, these fungi provide a rather unique and relatively easy-to-manipulate model system to further explore mechanisms controlling mitochondrial inheritance.

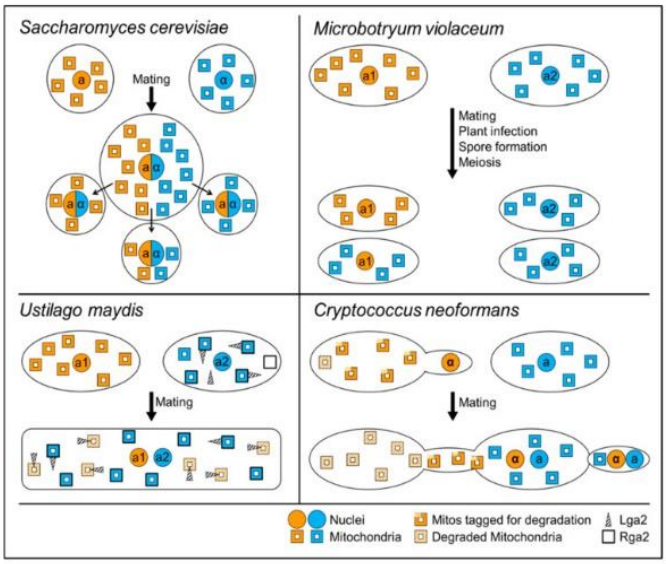

Figure 2. - Mechanisms of mitochondrial inheritance in fungi. (A) In *S. cerevisiae*, a and α type mitochondria remain relatively evenly distributed upon zygote formation. Whether offspring contain a or α type mitochondria or a mixture of both depends on the local position of the emerging bud. (B) In *U. maydis*, two proteins encoded in the a2 mating-type locus are responsible for uniparental mitochondrial inheritance. Rga2 shields mitochondria from the degradative effect of Lga2. Upon dikaryon formation, Lga2 leads to degradation of unprotected a1 type mitochondria. (C) In *M. violaceum*, sexual development results in offspring where a1 type cells contain either a1 or a2 type mitochondria and a2 type cells contain only a2 type mitochondria. The mechanism of this doubly uniparental inheritance pattern is unknown. (D) In *C. neoformans*, two effects might lead to uniparental mitochondrial inheritance. During pheromone stimulation, α type mitochondria might be tagged for degradation and be degraded during zygote formation. Only α type cells form conjugation hyphae through which the α type nuclei migrate into the zygotes. The zygote buds off at the opposite pole, thus further reducing the chance of inheriting α type mitochondria. Figure obtained, with permission, from Mendoza et al., 2020.

While mitochondrial inheritance mechanisms have been examined to some extent in *U. maydis*, such an examination in SRZ has not previously been undertaken. One prediction is that the a2 mating-type will dominate, but this hypothesis still needs to be tested experimentally. Here I provide a potential tool to conduct that experimental test.

2. Materials and Methods

2.1 Strains and Growth Conditions

Escherichia coli was grown in LB (1% Tryptone, 0.5% Yeast Extract, and 1% NaCl) media in a 37° C rotary shaker at 200 rpm for 12 to 24 hours. *E. coli* on solid LB plates were grown in an incubator until desired growth was achieved.

The strains of SRZ utilized in this research are listed in Table 1. Haploid strains were grown in potato dextrose (PD) broth in a 28° C rotary shaker at 200 rpm until an absorbance at 600 nm (OD or A_{600}) of 1 was achieved on a spectrophotometer. Strains on solid PD agar plates were grown in an incubator at 28° C for two days until optimal growth was achieved and then stored in a refrigerator at 4° C. Transgenic strains were maintained by adding hygromycin or carboxin at a concentration of 100 μg/mL or 5 μg/mL, respectively, to the PD medium.

Table 1. SRZ Strains

Name	Mating type	Characteristics
5-1 WT	*a2b2*	Wild type
5-1 eGFP #2	*a2b2*	Green fluorescence
5-1 mCherry #2	*a2b2*	Red fluorescence
5-2 WT	*a1b1*	Wild type
5-2 eGFP #6	*a1b1*	Green fluorescence
5-2 eGFP #7	*a1b1*	Green fluorescence

2.2 DNA Isolation

For *E. coli* DNA isolation, the bacterium was inoculated into 4 mL Circlegrow media (MP Biomedicals) and grown overnight with shaking at 37° C. A plasmid isolation was then performed using a Zymo Research DNA Miniprep Kit (Zymo Research, Irvine, CA).

For fungal DNA isolation, the strain was inoculated into 4 mL PD broth and shaken overnight at 28° C. Fungal genomic DNA was isolated to confirm the incorporation of the

desired fragment into the genome. The DNA extraction was performed using PCI (25 phenol:24 chloroform: 1 isoamyl alcohol) followed by one 100% ethanol precipitation and two 70% ethanol wash steps. After precipitation, samples were dried via suction with a vacuum pump, and TE (10 mM Tris/1mM EDTA, pH 8.0) was used to resuspend the pellet and increase the stability of the DNA (Hoffman, 1987).

2.3 PCR Protocol

Polymerase chain reaction (PCR) was used to amplify target regions of the fungal genomic DNA, including the up and down flanks surrounding the *aox* gene. PCR also allowed amplification of other DNA fragments necessary for plasmid construct generation. The reactions were performed in a T100 ThermalCycler (Bio-Rad Laboratories, Hercules, CA, USA). Ex Taq Hot Start DNA Polymerase (TaKaRa Bio USA, Inc., San Jose, CA, USA), PrimeSTAR Max DNA Polymerase (TaKaRa Bio USA, Inc., San Jose, CA, USA), or Dream-Taq Hot Start PCR Master Mix(Thermo Fisher Scientific, Waltham, MA, USA) were used for the reaction. PCR cycling conditions for Hot Start DNA polymerases involved an initial denaturation step at 94° C for 4 minutes. Next, the samples went through 35 cycles of a three-step process. The steps were denaturation at 94° C lasting 30 seconds, extension at 72° C for 1 minute per 1 kilobase pair (kbp) of anticipated DNA product, and a final extension step at 72° C lasting 10 minutes. PCR cycling conditions for Dream-Taq Hot Start PCR master mix closely mirrored those of Ex Taq Hot Start DNA Polymerase. PCR cycling conditions for PrimeSTAR Max DNA Polymerase involved an initial denaturation step at 98° C lasting two minutes followed by 35 cycles of a three-step process. The steps were denaturation at 98° C lasting 10 seconds, annealing at 58-62° C lasting 15 seconds, and extension at 72° C lasting 30-45 seconds. After the cycling, a final

extension occurred at 72° C which lasted 5 minutes. Primers necessary during Gibson overlap, transformant screening, and screening for targeted insertion are located in Table 2.

Table 2. PCR Primers

Primer Name	Sequence	Use (Relevant Figure)
oHM34 - Sr AOX Hyg 1507 R	5'- AGTTCGATTCTGTGGAATTGTGAGCGGATA-3'	Gibson Reaction
oHM37 - Sr AOX Down F	5'- CAATTCCACAGAATCGAACTGGCGAATGTC-3'	Gibson Reaction
oHM38 - Sr AOX Down R	5'-TTCAATATTAATTAAAGGTGATGAAGGAACGAACG-3'	Gibson Reaction
oHM39 - Sr AOX Ori+Amp R	5'- CATGCTTGATATCAAAAGGCCGCGTTGCTG-3'	Gibson Reaction
oHM40 - Sr AOX Ori+Amp F	5'- ATCACCTTTAATTAATATTGAAAAAGGAAGAG-3'	Gibson Reaction
oHM61 - SRZ AOX qRT F	5'- GAAAAGACCGTGGCTCTCC-3'	qRT-PCR
oHM62 - SRZ AOX qRT R	5'- GTGCTTCACTGGCATCGTC-3'	qRT-PCR
oHM70 - SRZ AOX GFP Up F	5'- TTTTGATATCCGACTTTTCGGGTGATTTTC-3'	Gibson Reaction
oHM102 - SRZ AOX eGFP F	5'- GAAGACCGCCATGGTGAGCAAGGGCGAG-3'	Gibson Reaction
oHM103 - SRZ AOX eGFP R	5'- CGTCGTTTTATTCTTGTGATTCGGGGACTC-3'	Gibson Reaction
oHM104 - SRZ AOX eGFP Up R	5'- TGCTCACCATGGCGGTCTTCTCAGCAGC-3'	Gibson Reaction
oHM105 - SRZ AOX eGFP Hyg F	5'- ATCACAAGAATAAAACGACGGCCAGTGAAT-3'	Gibson Reaction
oHM106 - SRZ AOX mCherry R	5' - CGTCGTTTTACCGCAATTCTCATGTTTGAC-3'	Gibson Reaction
oHM107 - SRZ AOX mCherry Hyg F	5' - AGAATTGCGGTAAAACGACGGCCAGTGAAT-3'	Gibson Reaction
oHM108 -mCherry qRT F	5'- GACCACCTACAAGGCCAAGA-3'	qRT-PCR
oHM109 - mCherry qRT R	5'- GTGGGAGGTGATGTCCAACT-3'	qRT-PCR
oYZ58 - GAPDH	5'- GGATTTCATCGGCAACTCAC-3'	qRT-PCR
oYZ59 - GAPDH	5'- TACCACGAGACGAGCTTGAC-3'	qRT-PCR

2.4 RT-qPCR Protocol

Two-step reverse transcription quantitative PCR (RT-qPCR) confirmed the incorporation of the construct into the fungal genome. Fungal nucleic acids were isolated from SRZ haploid sporidia grown on PD plates via homogenization in a frozen mortar and pestle followed by treatment with TRIzol reagent (Invitrogen, Waltham, MA, USA). RNA was then isolated using a Direct-zol RNA Miniprep Kit (Zymo, Irvine, CA, USA). First-strand cDNA was generated from

purified RNA using a Superscript IV protocol (Thermo Fisher, Waltham, MA, USA) and then utilized in subsequent reactions. The reaction was performed in a StepOne thermal cycler (Applied Biosystems, Foster City, CA, USA) using Evagreen fluorescent dye (Biotium, Fremont, CA, USA) following the manufacturer's instructions. RT-qPCR cycling conditions involved an initial denaturation step at 95° C which lasted 10 minutes followed by 40 cycles at 95° C lasting 15 seconds and 60° C lasting 1 minute.

2.5 Construct Creation and Digestion

In order to generate fluorescent strains with a microscopically visible phenotype, a construct was designed that incorporated a fluorescent protein (mCherry or eGFP) to cause fluorescence, an antibiotic (Hygromycin) that would allow for selection of transformed SRZ and easy confirmation of gene insertion along with upstream and downstream flanking regions to *aox*. These three pieces together would allow for the insertion of a gene to replace *aox* present in the genome, but first, they needed to be combined. This was accomplished in *E. coli* and required the additional pieces of an ampicillin resistance gene along with an origin of replication, amplified from a standard plasmid vector, pUC19 (Norrander 1983). With all these pieces, the full construct could be ligated together using a single Gibson reaction.

The Gibson reaction (Gibson, 2009) utilizes an exonuclease capable of creating single stranded 3' overhangs. Those fragments with compatible overhang regions are then annealed together to create one strand. The gaps in the strand are finally fixed by a DNA polymerase to result in one fully connected strand of DNA. For these reactions, I used a commercially available kit (NEBuilder® HiFi DNA Assembly Master Mix, New England Biolabs, Ipswich, MA) according to the manufacturer's instructions.

The primer pair oHM39/40 was used to generate a single fragment containing the cassette for ampicillin resistance along with the origin of replication element. The template for this fragment was pUC19 DNA. The primer pair oHM70/104 and oHM37/38 were used to create upstream and downstream flanking regions to *aox*. The template for these fragments was SRZ DNA. This upstream *aox* coding sequence notably does not contain a STOP codon, this allows for the completed plasmid to be fully translated from the *aox* coding region through the fluorescent gene; the antibiotic resistance gene carries its own separate promoter. The primer pair oHM102/103 was used to generate a fragment containing eGFP from pMF4-1c DNA (Brachmann, 2004), and the primer pair oHM102/106 was used to generate a fragment containing mCherry from pMF5-5h DNA (https://www.mikrobiologie.hhu.de/en/ustilago-community/types-of-genetic-engeneering/55-c-terminal-fusion-with-mcherry-and-triple-myc/pmf5-5h-with-hygromycin-resistance-cassette; kindly provided by M. Feldbrügge). The primer pair oHM34/105 was used to generate the hygromycin resistance cassette from pUMA1507 DNA (Terfrüchte, 2014). These fragments were then ligated together in a single Gibson reaction. The resulting sample of DNA was then used for transformation into *E. coli* by heat shock.

The plasmid DNA was then isolated from the *E. coli* and digested using EcoRV (New England Biolabs, Ipswich, MA, USA) to create a linear strand. Next, the primer pair oHM38/70 was used to amplify the *aox-eGFP* fusion construct (6835 bp) containing the flanking upstream region of *aox* without the STOP codon, followed by the eGFP fragment, the hygromycin resistance cassette, and the downstream flanking region. The amplified construct was then used in the transformation of 5-1 and 5-2 strains of SRZ through homologous recombination during Polyethylene Glycol (PEG) transformation. The primer pair oHM38/70 was also used to amplify

the *aox-mCherry* fusion construct (6929 bp). This second construct with mCherry mirrored the eGFP construct in every way except for bp size and a difference in fluorescent protein (mCherry).

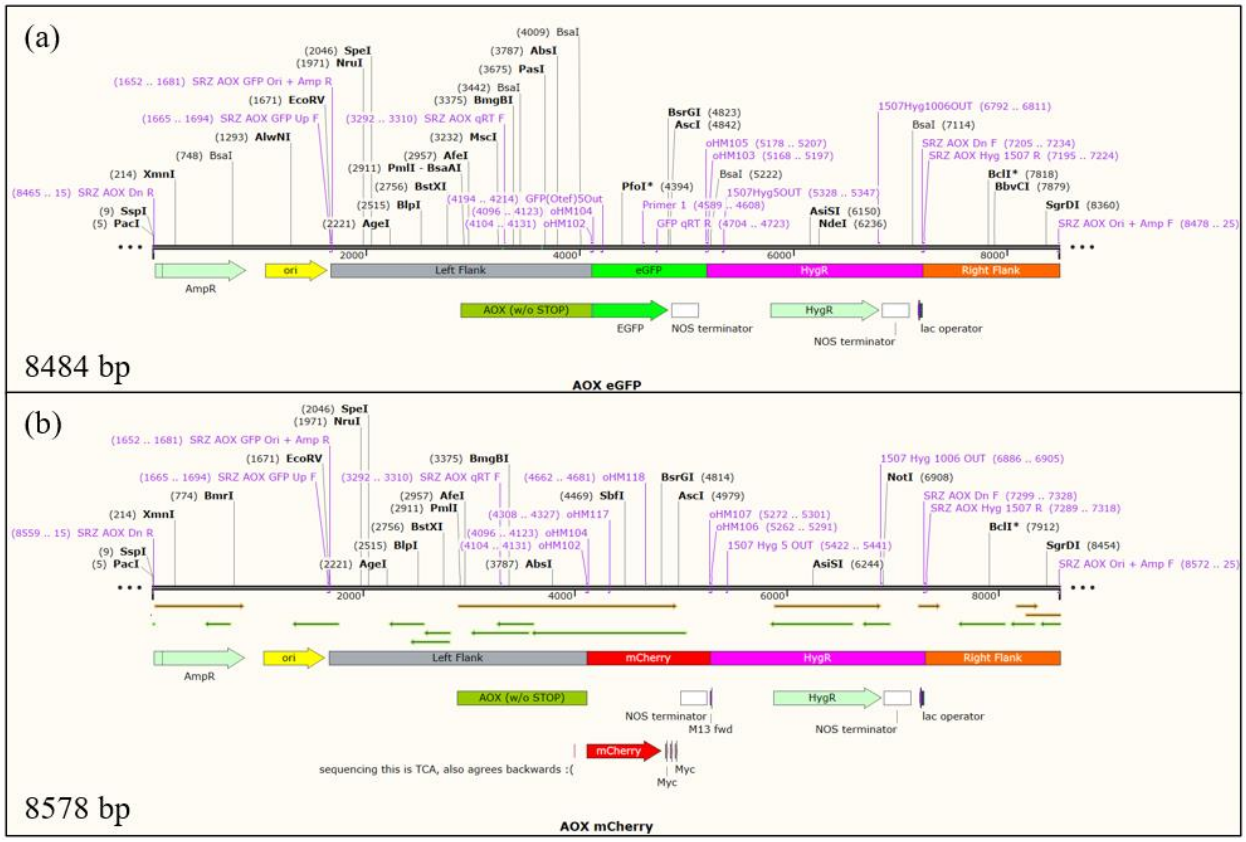

Figure 3. Linear construct for eGFP and mCherry assembled via Gibson overlap. *E. coli* transformants were selected on ampicillin plates (LB agar containing 200 μg ampicillin per ml agar). The Hyg^R section of the construct ensures selection was only for potential SRZ transformants.

2.6 Polyethylene Glycol (PEG) Transformations

SRZ transformations were performed using protoplasts from two mating types (5-1 and 5-2). Transformations were performed using protoplasts: fungal cells with their cell walls removed. This absence of the cell wall allows for DNA to more easily enter the cell. The protoplasts were generated using Novozyme (2.5 mg/mL; Sigma-Aldrich), which enzymatically

stripped the cell wall and allowed DNA to enter the cell while maintaining the ability of the cell to regenerate its cell wall on appropriate hypertonic medium (*e.g.*, containing 1 M sucrose). The construct generated from Gibson overlap was transformed into SRZ by plating a STC-polyethyleneglycol mixture with the protoplasts and construct DNA onto YPS PD plates containing hygromycin B (100-200 μg/mL). Plates were then incubated for approximately a week at 28° C before colonies were sub-cultured onto fresh PD plates containing hygromycin B.

2.7 Transformant Confirmation

Potential transformants were identified by their growth on 100-200 μg/mL hygromycin plates. Colonies that continued to grow were suspected to be transformants containing the gene for hygromycin resistance and thus the fluorescent tag on the *aox* gene as well. Those strains were then streaked onto PD plates without antibiotic. They were inoculated into 4 mL PD broth and their DNA was isolated and screened with PCR using oHM34/102 for eGFP and mCherry strains to check for proper insertion of the construct into the genome. Gel electrophoresis was then performed to confirm the presence of a band of the appropriate expected sizes. Wild type strain negative controls showed no bands since they do not contain the construct.

2.8 Microscopy and Strain Crosses

Transformed SRZ strains were grown for 12 hours at 28° C in PD broth to an A_{600} of 1. The SRZ strains were then crossed, where 5-1 #2 eGFP was mated with 5-1 #2 mCherry, 5-1 #2 mCherry was mated with 5-2 #6 eGFP, and 5-1 #2 mCherry was mated with 5-2 #7 eGFP. The crossed strains were then grown until hyphal development was observed using light microscopy.

Ten-fold dilutions of strain cultures were made, which included 450 μL PD Broth and 50 μL cell media. This mixture was pipetted into the wells of 35-mm CELLview Culture Dishes (Greiner Bio-One, Monroe, NC, USA) to prepare for confocal microscopy.

Cell images were captured with an Olympus-CH series light microscope to confirm cell visibility and concentration after 12 hours of growth. Additional images were captured after mating the respective strains to confirm mating between compatible mating type partners.

Fluorescence images were acquired using a Nikon A1R confocal microscope. eGFP signal was observed using a 488 nm line of an Argon laser and was detected at 510 nm. The mCherry signal was detected at 521 nm. A transmitted light image was acquired for better visualization of cell outline by grouping of the transmitted detector with the argon laser. To confirm the localization of the fluorescently tagged Aox proteins, cells were treated with 100 μM MitoView Blue (Biotium, Fremont, CA 94538, USA) for 10 minutes. Blue fluorescence was acquired using the DAPI detection channel and overlapped with eGFP fluorescence.

3. Results

The eGFP and mCherry fusion constructs (Figure 3) were added to the genomes of SRZ 5-1 (*a2b2*) and 5-2 (*a1b1*). Primer pair oHM38/70 was used to amplify the target regions from isolated DNA of the strains via PCR and confirm the presence of the construct. The transformants showed a band of approximately 6835 bp and 6929 bp for eGFP and mCherry, respectively, due to the presence of the hygromycin resistance gene and fluorescent protein gene, while wild type negative controls not containing the construct showed no band. An agarose gel image demonstrating these bands for two of the strains used for this research isshown in Figure

4. Additionally, qRT-PCR was used to further confirm the proper assembly of the construct and expression of the involved proteins.

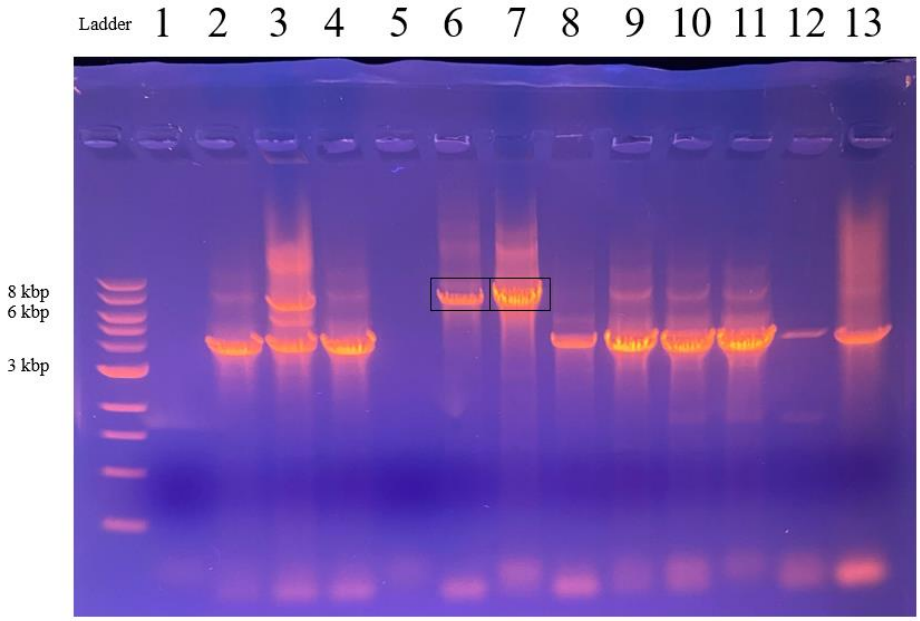

Figure 4. Example of agarose gel run to demonstrate the presence of *eGFP* and hygromycin resistance gene incorporation into the genome. In this case, the 6th and 7th lanes show bands at approximately 7000 bp which is an expected band size for the construct fragment. Every other band was unclear or could have been the result of insertion into the wrong location.

Following PEG transformation, PCR amplification and qRT-PCR confirmation, four potential transformants were fully screened, and demonstrated evidence of proper construct incorporation. These were 5-1 eGFP #2 and mCherry #2 along with 5-2 eGFP #6 and #7. The cells were then viewed under a light microscope and observed to grow successfully via budding with no noticeable changes as compared to wild type strains. Next, confocal microscopy was performed on the first of the transformants to be fully screened, 5-1 #2 eGFP, an image of which can be seen in Figure 5.

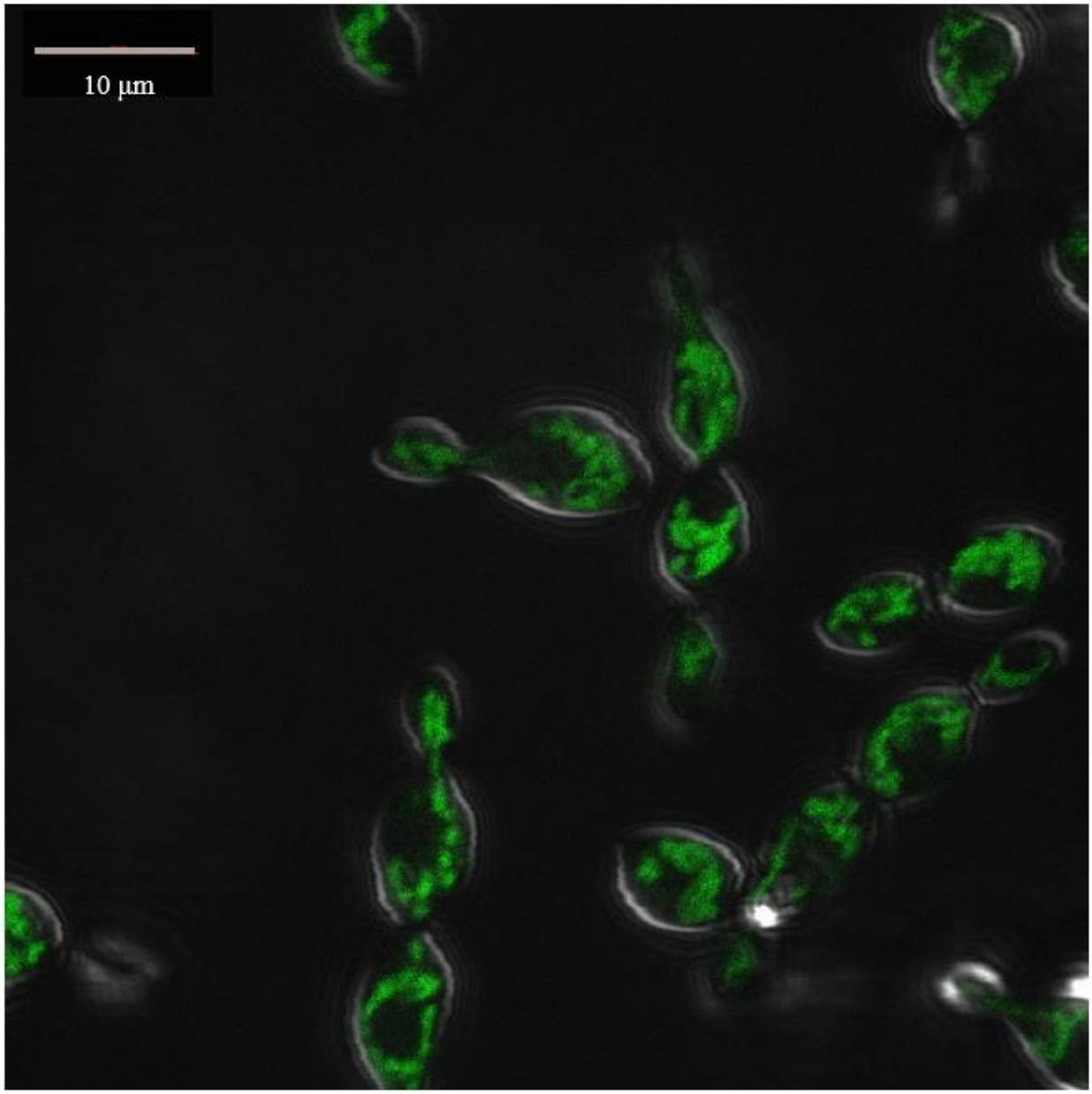

Figure 5. Confocal microscopy of transformed 5-1 #2 eGFP SRZ cells containing the *aox-eGFP* fusion construct. The presence of the fusion construct makes the thin thread-like mitochondria visible within the budding cells.

Additional confocal microscopy images were captured in order to confirm that this detected fluorescence resulted from the mitochondria. Cells were treated with a mitochondrial fluorogenic dye called MitoView Blue, which has a light absorbance and emission at 398 nm and 440 nm, respectively. It is capable of penetrating membranes and localizes to the mitochondrial

membrane where it gives off bright blue fluorescence. Overlap between MitoView Blue fluorescence and green fluorescence from eGFP would indicate that the green fluorescent structures are mitochondria and that proper localization of the tagged Aox protein into the inner membrane of the mitochondria occurred. Figure 6 shows overlapping and individual images of SRZ 5-1 #2 eGFP cells fluorescence.

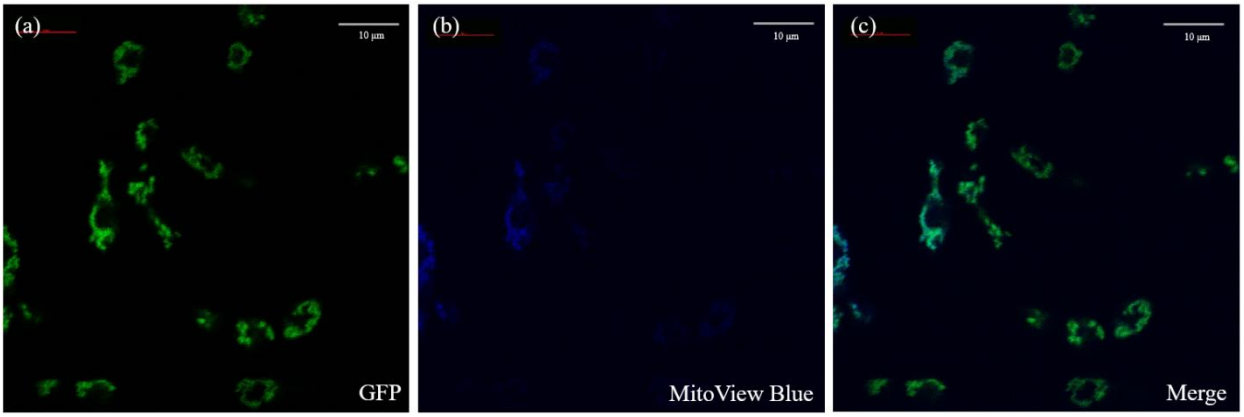

Figure 6. Confocal microscopy confirmation of Aox localization in 5-1 #2 SRZ cells. **(a)** eGFP fluorescence. **(b)** MitoView Blue fluorescence. **(c)** Merged green and blue fluorescence. Size bar, 10 µm.

With one strain fully confirmed and visible using confocal microscopy, the other eGFP strains in the opposite mating type along with the mCherry strain (5-1 #2 mCherry) were confirmed as well with confocal microscopy. 5-1 #2 mCherry confocal microscopy images are shown in Figure 7.

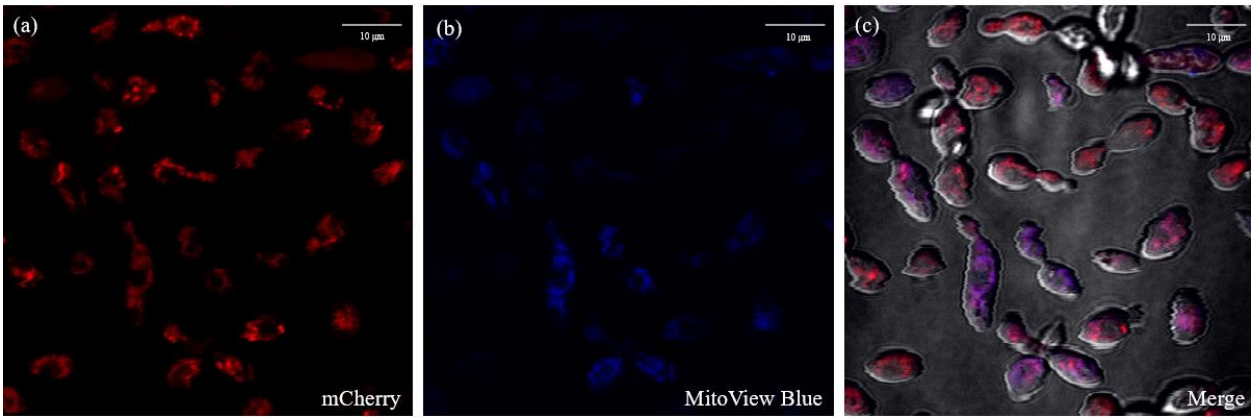

Figure 7. Confocal microscopy and confirmation of Aox localization using 5-1 #2 mCherry SRZ cells containing the *aox-mCherry* fusion construct. **(a)** mCherry fluorescence. **(b)** MitoView Blue fluorescence. **(c)** Merged red and blue fluorescence. Size bar, 10 µm.

With all four strains visible using confocal microscopy, different mating types were crossed in an attempt to capture confocal microscopy images of SRZ mating. Some of the results of this experiment are shown in Figure 8. Images appeared to only display budding and not sexual reproduction between opposite mating types. This conclusion is due to the identical appearance of cells present in the crosses between 5-1 and 5-2 strains as compared with the control containing 5-1 #2 eGFP and 5-1 #2 mCherry strains alone. The plate with only 5-1 strains would not show mating due to both having the same *a2b2* mating loci.

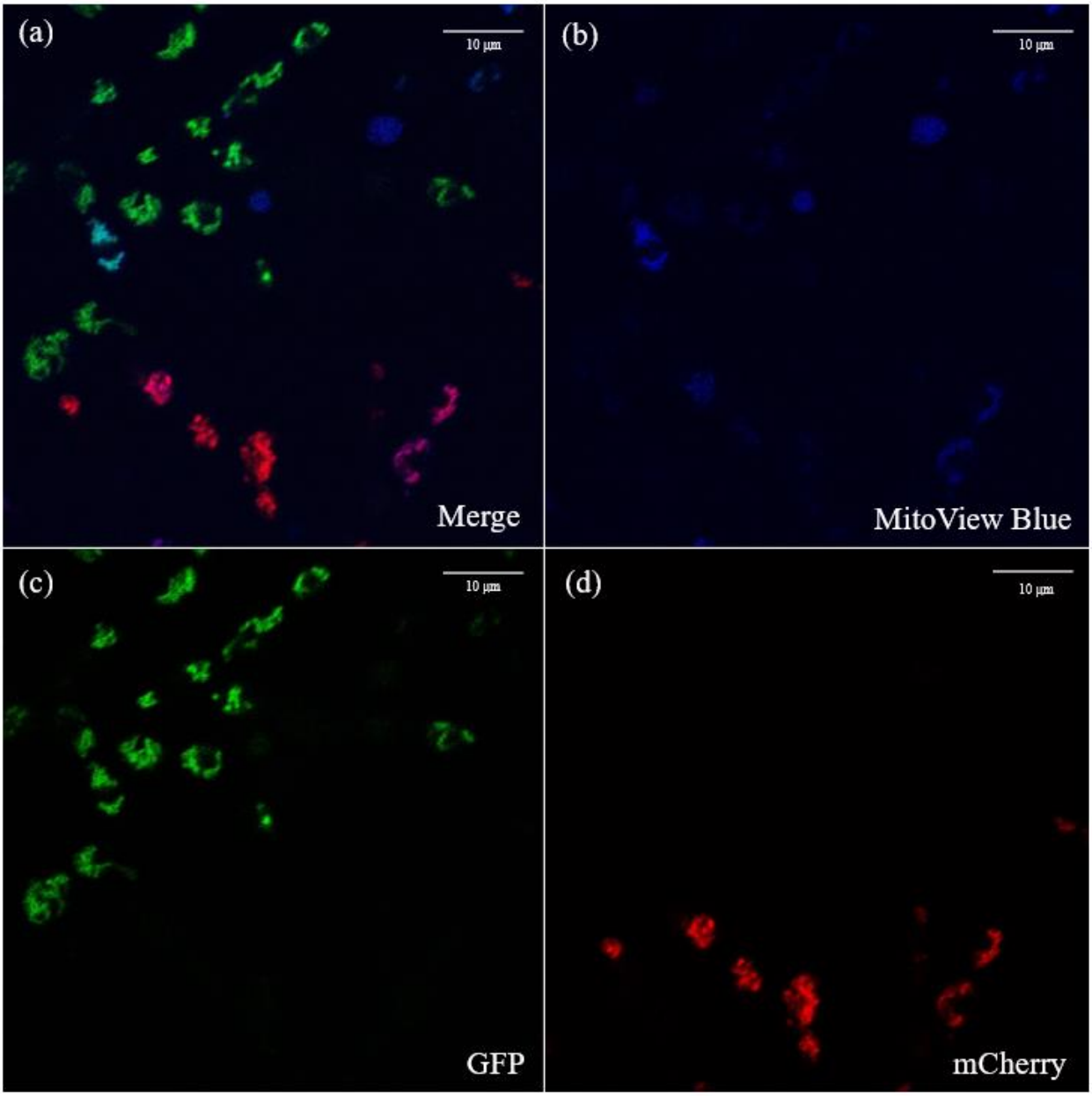

Figure 8. Confocal microscopy of transformed 5-1 #2 and 5-2 #7 cells containing the *aox-mCherry* and *aox-eGFP* fusion constructs, respectively. Confirmation of Aox localization in SRZ. **(a)** merged eGFP, mCherry and MitoView blue fluorescence, **(b)** MitoView Blue fluorescence, **(c)** eGFP fluorescence of 5-1 #2 eGFP alone, **(d)** mCherry fluorescence of 5-1 #2 mCherry alone. Size bar, 10 µm.

These results show the presence of both 5-1 and 5-2 cells in the same region along with confirmation of proper localization thanks to the MitoView Blue stain. However, mating was not

suspected to have occurred due to the identical appearance between the plates containing the opposite mating partners and the control plate containing two strains with the same mating type.

Following these results, additional images were taken after new strategies were implemented during confocal microscopy plate preparation to ensure mating between opposite SRZ mating types. These alterations to the original protocol resulted in the SRZ images displayed in Figure 9.

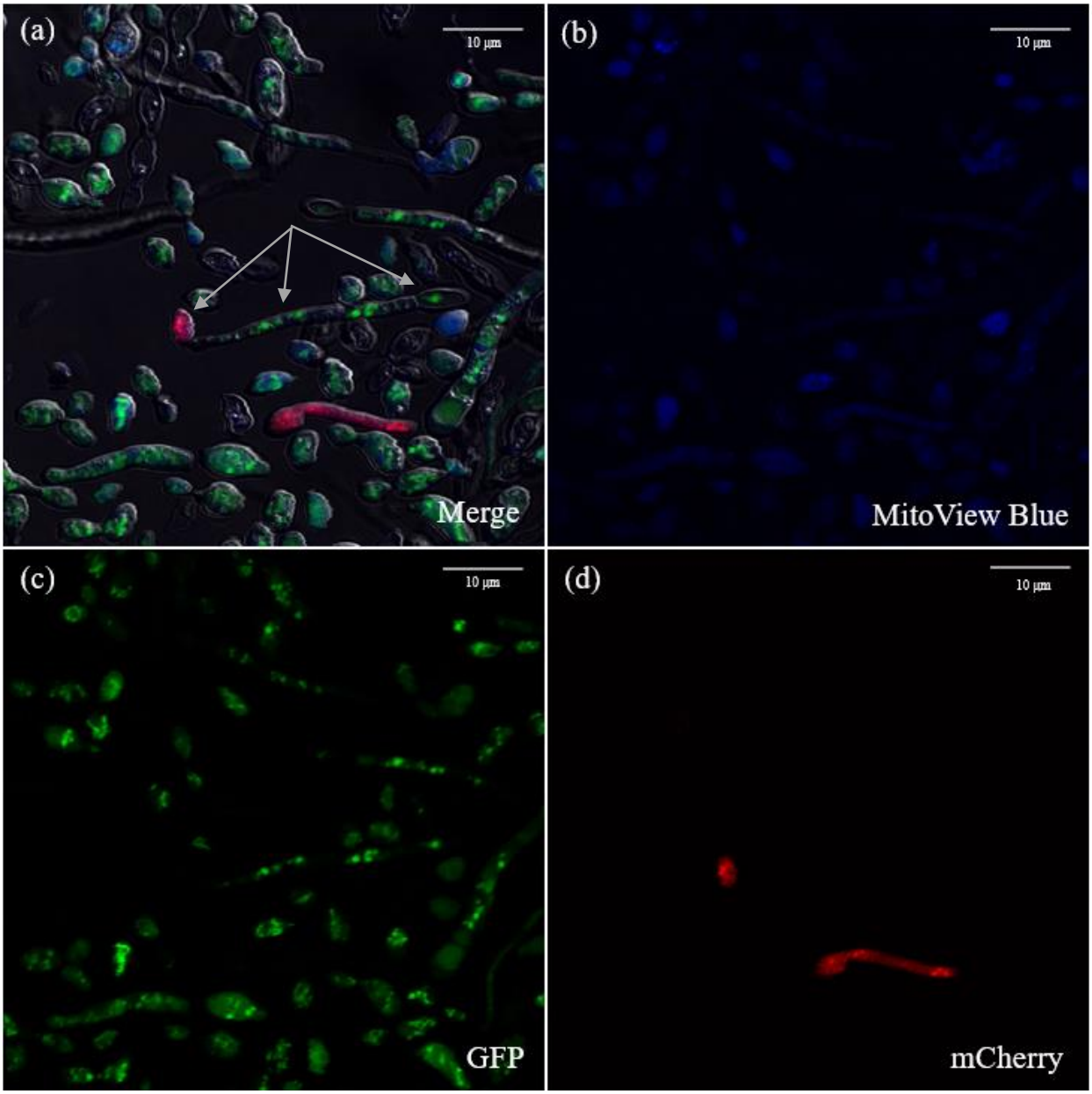

Figure 9. Confocal microscopy of crossed 5-1 mCherry #2 and 5-2 eGFP #6 strains containing the *aox-mCherry* and *aox-eGFP* fusion constructs, respectively. The grey arrows indicate from left to right: a 5-1 mCherry #2 cell, a hyphal filament from a 5-2 eGFP #6 cell, and a 5-2 eGFP #6 cell. Confirmation of Aox localization in SRZ. **(a)** merged eGFP, mCherry and MitoView blue fluorescence. **(b)** MitoView Blue fluorescence. **(c)** eGFP fluorescence. **(d)** mCherry fluorescence. Size bar, 10 µm.

4. Discussion

This study utilized Aox, an alternative component of the ETC found in plants and some fungi, as a way to tag mitochondria of the fungus, *S. reilianum* f. sp. *zeae*. Aox normally resides in the inner membrane of mitochondria, and fluorescently labelled Aox proteins would thereby be a useful tool in following mitochondrial inheritance after mating of haploid cells. In these experiments, incorporation of the genes encoding eGFP or mCherry fluorescent proteins and a hygromycin resistance gene was achieved in two SRZ haploid strains: 5-1 and 5-2. Proper incorporation of these elements of the constructs was confirmed via PCR and RT-qPCR (results not shown) to ensure proper expression of the genes. Confocal microscopy allowed for visualization of the mitochondria in the four transgenic strains of SRZ. The 5-1 mCherry #2 strain fluoresced red and the 5-1 eGFP #2, 5-2 eGFP #6, and 5-2 eGFP #7 strains fluoresced green. MitoView Blue stain allowed for confirmation that the mitochondria were in fact fluorescing and that red or green fluorescence was not occurring in other parts of the cell. This further supports the findings of Mendoza et al. (2022) performed previously with 5-1 eGFP #2 strain.

Four rounds of confocal microscopy were performed. The first and second rounds of confocal microscopy served to confirm the localization of the fluorescently tagged Aox to the mitochondria. The third and fourth rounds attempted to observe sexual reproduction between mating types. During the third round, the confocal microscopy images from the crosses between 5-1 and 5-2 strains, along with a negative control of 5-1 and 5-1 strains all appeared identical. This similarity in appearance and lack of hyphal development indicated sexual reproduction had not yet occurred between the 5-1 and 5-2 mating partners under the conditions and time period initially employed. In order to remedy this issue and encourage reproduction between mating partners, the shaking and incubation period at 28° C was extended to 72 hours from the 12 hours

normally used. This alteration encouraged the cells to switch from their budding stage and begin searching for a mating partner due to a loss of nutrients in the PD broth. The more the strains grew, the more nutrients were depleted, which increased the chance of the haploid cells switching to sexual reproduction as an alternative to axenic growth and, normally, as a prelude to infection of its host.

For the fourth round of confocal microscopy, these changes in protocol led to the image in Figure 9 that appears to sow fusion between a 5-1 mCherry #2 cell and a 5-2 eGFP #6 cell. While the production of a dikaryon was not observed, fusion of the membranes indicates that reproduction is possible and may yet be visualized between the fluorescently tagged cells.

Conclusions and Limitations

The goal of this study was to investigate mitochondrial inheritance in SRZ through the use of fluorescently tagged Aox protein (with either eGFP or mCherry fluorescent proteins). This provided a method to microscopically distinguish mitochondria from one mating-type partner, both before, during, and after mating. Four strains of SRZ (two in the 5-1 mating type and two in the 5-2 mating type) were fluorescently tagged with eGFP and mCherry and those tagged strains exhibited normal growth as compared to WT 5-1 and 5-2 strains, thus demonstrating that the tagged versions of Aox were not altered in their functions/roles in the ETC. Confocal microscopy was used to document the fluorescently tagged mitochondria and MitoView Blue staining was used to confirm that the detected fluorescence indicated localization specifically to the mitochondria. Confocal microscopy did indicate that these strains possess fluorescent mitochondria due to the presence of tagged Aox in the inner mitochondrial membrane of the fungal cells. Fusion of the mating partners through a hyphal filament was also observed,

however, only a few cells exhibited fusion even though many were filamenting (a sign the cell is searching for an opposite mating partner).

One possible reason for the lack of full dikaryon development and later steps of sexual reproduction could be the use of liquid media in this research. SRZ may prefer to undergo sexual reproduction on a plant host, which could be tested through further studies utilizing infected host plants. The use of PD or water agar plates would also more closely mimic a host plant as compared to a liquid environment. Samples could be grown on plates and then inoculated into liquid (*e.g.*, water or buffer) for confocal microscopy.

Additionally, more strains of fluorescently tagged SRZ will be needed in order to fully ascertain the mitochondrial inheritance patterns in offspring. Time was a limiting factor in this regard due to the difficulty of generating fluorescent strains. SRZ CXI strains with the a3 mating locus were not tagged and thus further mitochondrial inheritance experiments could not be performed. With fluorescent CXI strains, a more complete understanding of mitochondrial inheritance between mating partners with the a1 and a3 mating loci could eventually be achieved.

Acknowledgements

This work was supported in part by an NSF/IRES award #1824851 to the Perlin lab. I cannot thank Dr. Michael Perlin enough for his mentorship during this project and the invitation he gave me four years ago to come to a Friday lab meeting. This work would also not be possible without Hector Mendoza, whose guidance, attention to detail, planning, thoughtfulness, and support allowed me to finish the project. Additional thanks go to Clinton Belott and David

Grimm from the Menze lab for volunteering their time to capture confocal microscopy images with me.

References

Banuett, F., & Herskowitz, I. (1994). Morphological Transitions in the Life Cycle of Ustilago maydis and Their Genetic Control by the a and b Loci. Experimental Mycology, 18(3), 247- 266. doi: 10.1006/emyc.1994.1024

Basse C. W. (2010). Mitochondrial inheritance in fungi. *Current opinion in microbiology*, *13*(6), 712–719. https://doi.org/10.1016/j.mib.2010.09.003

Bortfeld, M., Auffarth, K., Kahmann, R., & Basse, C. W. (2004). The Ustilago maydis a2 mating-type locus genes lga2 and rga2 compromise pathogenicity in the absence of the mitochondrial p32 family protein Mrb1. *The Plant cell*, *16*(8), 2233–2248. https://doi.org/10.1105/tpc.104.022657

Brachmann, A., König, J., Julius, C., & Feldbrügge, M. (2004). A reverse genetic approach for generating gene replacement mutants in *Ustilago maydis*. *Molecular genetics and genomics : MGG*, *272*(2), 216–226. https://doi.org/10.1007/s00438-004-1047-z

Cárdenas-Monroy CA, Pohlmann T, Piñón-Zárate G, Matus-Ortega G, Guerra G, Feldbrügge M, et al. (2017) The mitochondrial alternative oxidase Aox1 is needed to cope with respiratory stress but dispensable for pathogenic development in *Ustilago maydis*. PLoS ONE 12(3): e0173389. https://doi.org/10.1371/journal.pone.0173389

Dinakar, C., Vishwakarma, A., Raghavendra, A. S., & Padmasree, K. (2016). Alternative Oxidase Pathway Optimizes Photosynthesis During Osmotic and Temperature Stress by Regulating Cellular ROS, Malate Valve and Antioxidative Systems. *Frontiers in plant science*, *7*, 68. https://doi.org/10.3389/fpls.2016.00068

Fedler, M., Luh, K. S., Stelter, K., Nieto-Jacobo, F., & Basse, C. W. (2009). The a2 mating-type locus genes lga2 and rga2 direct uniparental mitochondrial DNA (mtDNA) inheritance and constrain mtDNA recombination during sexual development of Ustilago maydis. *Genetics*, *181*(3), 847–860. https://doi.org/10.1534/genetics.108.096859

Gibson, D. G., Young, L., Chuang, R. Y., Venter, J. C., Hutchison, C. A., 3rd, & Smith, H. O. (2009). Enzymatic assembly of DNA molecules up to several hundred kilobases. *Nature methods*, *6*(5), 343–345. https://doi.org/10.1038/nmeth.1318

Giles, R. E., Blanc, H., Cann, H. M., & Wallace, D. C. (1980). Maternal inheritance of human mitochondrial DNA. *Proceedings of the National Academy of Sciences of the United States of America*, *77*(11), 6715–6719. https://doi.org/10.1073/pnas.77.11.6715

Grabelnych, O. I., Borovik, O. A., Tauson, E. L., Pobezhimova, T. P., Katyshev, A. I., Pavlovskaya, N. S., Koroleva, N. A., Lyubushkina, I. V., Bashmakov, V. Y., Popov, V. N., Borovskii, G. B., & Voinikov, V. K. (2014). Mitochondrial energy-dissipating systems (alternative oxidase, uncoupling proteins, and external NADH dehydrogenase) are involved in development of frost-resistance of winter wheat seedlings. *Biochemistry. Biokhimiia*, *79*(6), 506–519. https://doi.org/10.1134/S0006297914060030

Juárez, O., Guerra, G., Martínez, F., & Pardo, J. P. (2004). The mitochondrial respiratory chain of Ustilago maydis. *Biochimica et biophysica acta*, *1658*(3), 244–251. https://doi.org/10.1016/j.bbabio.2004.06.005

Juárez, O., Guerra, G., Velázquez, I., Flores-Herrera, O., Rivera-Pérez, R. E., & Pardo, J. P. (2006). The physiologic role of alternative oxidase in Ustilago maydis. *The FEBS journal*, *273*(20), 4603–4615. https://doi.org/10.1111/j.1742-4658.2006.05463.x

Hoffman, C., & Winston, F. (1987). A ten-minute DNA preparation from yeast efficiently releases autonomous plasmids for transformation of Escherichia coli. Gene, 57(2-3), 267-272. doi: 10.1016/0378-1119(87)90131-4

Mann J. L. (1983). Autofluorescence of fungi: an aid to detection in tissue sections. *American journal of clinical pathology*, *79*(5), 587–590. https://doi.org/10.1093/ajcp/79.5.587

Martinez, C., Roux, C., Jauneau, A., & Dargent, R. (2002). The Biological Cycle of Sporisorium reilianum f.sp. zeae: An Overview Using Microscopy. *Mycologia, 94*(3), 505-514. doi:10.2307/3761784

Mendoza, H., Perlin, M. H., & Schirawski, J. (2020). Mitochondrial Inheritance in Phytopathogenic Fungi-Everything Is Known, or Is It?. International journal of molecular sciences, 21(11), 3883. https://doi.org/10.3390/ijms21113883

Mendoza H, Culver CD, Lamb EA, Schroeder LA, Khanal S, Müller C, Schirawski J, Perlin MH. Identification and Functional Characterization of a Putative Alternative Oxidase (Aox) in *Sporisorium reilianum* f. sp. *zeae*. *Journal of Fungi*. 2022; 8(2):148. https://doi.org/10.3390/jof8020148

Norrander, J., Kempe, T., & Messing, J. (1983). Construction of improved M13 vectors using oligodeoxynucleotide-directed mutagenesis. *Gene*, *26*(1), 101–106. https://doi.org/10.1016/0378-1119(83)90040-9

Pohlmann, T. pMF5-5h with hygromycin resistance cassette. https://www.mikrobiologie.hhu.de/ustilago-community/types-of-genetic-engeneering/55-c-terminal-fusion-with-mcherry-and-triple-myc/pmf5-5h-with-hygromycin-resistance-cassette

Rogov, A., Sukhanova, E., Uralskaya, L., Aliverdieva, D., & Zvyagilskaya, R. (2014). Alternative oxidase: Distribution, induction, properties, structure, regulation, and functions. Biochemistry (Moscow), 79(13), 1615-1634. doi: 10.1134/s0006297914130112

Schirawski, J., Heinze, B., Wagenknecht, M., & Kahmann, R. (2005). Mating type loci of Sporisorium reilianum: novel pattern with three a and multiple b specificities. *Eukaryotic cell*, *4*(8), 1317–1327. https://doi.org/10.1128/EC.4.8.1317-1327.2005

Smith, C. A., Melino, V. J., Sweetman, C., & Soole, K. L. (2009). Manipulation of alternative oxidase can influence salt tolerance in Arabidopsis thaliana. *Physiologia plantarum*, *137*(4), 459–472. https://doi.org/10.1111/j.1399-3054.2009.01305.x

Terfrüchte, M., Joehnk, B., Fajardo-Somera, R., Braus, G. H., Riquelme, M., Schipper, K., & Feldbrügge, M. (2014). Establishing a versatile Golden Gate cloning system for genetic engineering in fungi. *Fungal genetics and biology : FG & B*, *62*, 1–10. https://doi.org/10.1016/j.fgb.2013.10.012